

Smoothed Particle Hydrodynamics Simulations for Asteroid Deflection

Maximilian Rutz

Abstract

Contents

1	Introduction	3
2	Theory	5
2.1	Conservation equations	5
2.2	Constitutive equations	5
2.3	Equation of State	5
2.4	Porosity model	5
2.5	Fragmentation model	5
2.6	Strength model	6
3	Numerics	7
3.1	Smoothed Particle Hydrodynamics	7
3.1.1	Main SPH concepts	7
3.1.2	Smoothing kernel	8
3.1.3	Smoothing length	8
3.1.4	Artificial viscosity	8
3.2	Initial conditions	8
3.2.1	Particle setup	8
3.2.2	Material parameters	10
4	Results	12
4.1	Cratering	12
4.2	Beta factor	17
5	Discussion	21

1 Introduction

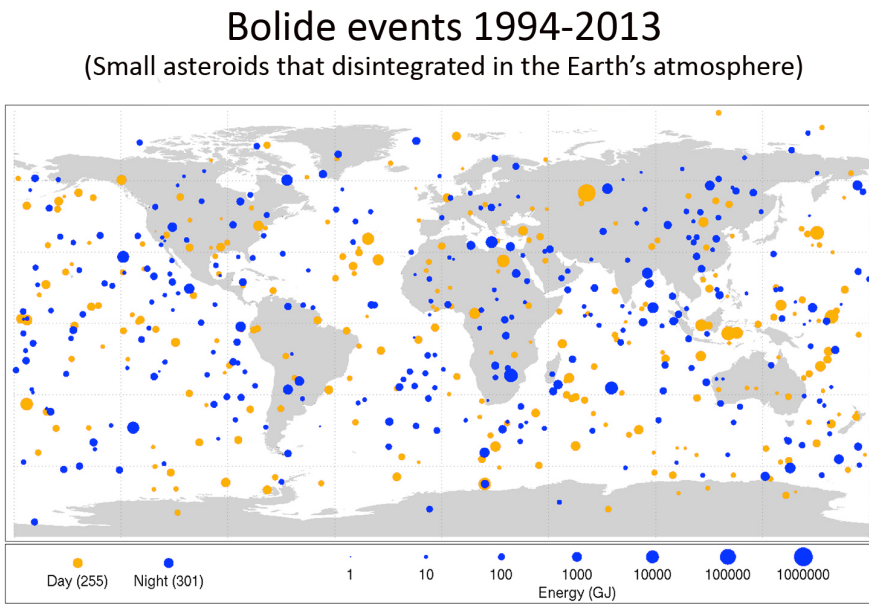


Figure 1: Past impacts [10]

- Dart and Hera Missions

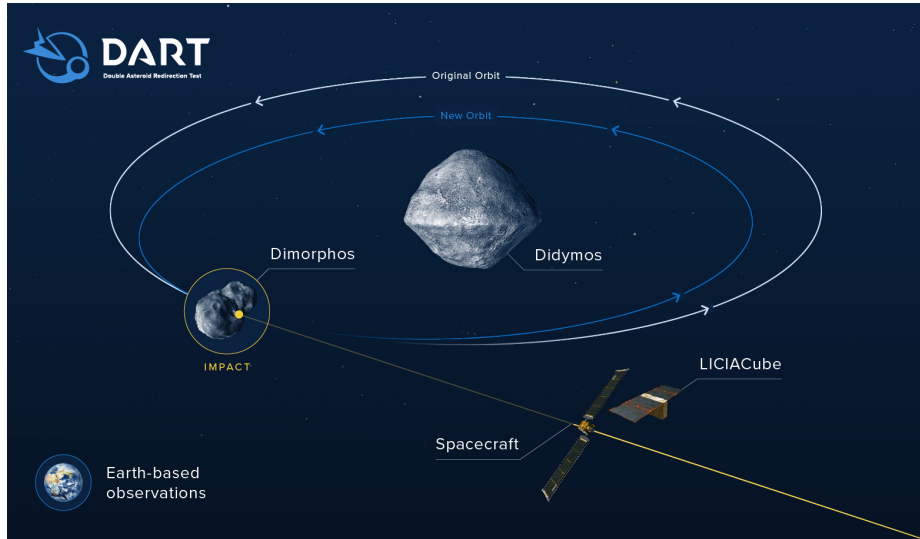


Figure 2: Dart mission [9]

Previous work: - Raducan [8] grid based 2d sims - Stickle [7] sph sims
 Improvement of previous work: - Effect of impact angle on beta factor
 Outline of the rest of the paper

2 Theory

- Equations from Geophysics/Continuum Mechanics and High velocity impact physics that are needed to model the Impact

- all parameters that appear in the table of the Numerics section should be explained

2.1 Conservation equations

- mass - momentum - energy

2.2 Constitutive equations

- time evolution of deviatoric stress tensor

2.3 Equation of State

- Tillotson equation of state [1]

2.4 Porosity model

There are different ways in which porosity can be modeled depending on the pore size. Depending on the simulation, macro porosity with pore sizes above the resolution of the simulation can be accounted for in the initial conditions. This however becomes impossible for granular material with sub-resolution sized grains and pores.

Microporosity models porosity as an additional material property and can be applied independently of the resolution.

In these simulations, a microporosity p- α model as outlined in [4] is used. The distention $\alpha \in [1, \infty)$ relates the current density ρ to the solid density ρ_s which is reached if the material is fully compressed. For a non-porous material α equals one.

$$\alpha \equiv \frac{\rho_s}{\rho} \quad (1)$$

Often the porosity ϕ is used instead of the distention α . They relate by

$$\phi = 1 - \frac{1}{\alpha} \quad (2)$$

- Quadratic crush curve

2.5 Fragmentation model

- fracture of brittle material - Weibull distribution

2.6 Strength model

- elastic and plastic regimes - von Mises strength - pressure dependent yield strength
 - ideas in [3] - implementation in [5]

3 Numerics

- how numerics are used to solve Equations from Theory section

3.1 Smoothed Particle Hydrodynamics

- before finite difference schemes with spherical coordinates - spherical coordinates bad for collisions

Smoothed Particle Hydrodynamics is a numerical simulation method first introduced by [2] in 1977. It is a Lagrangian particle method and as such often used when the geometry of the underlying problem makes it difficult to apply Eulerian grid-based methods like finite difference schemes. Although SPH is most often used to model liquids, it is possible to add physical models for solids as well.

- explanations apply to Miluphcuda

Miluphcuda is a smoothed particle hydrodynamics code that has been developed over several years at the University of Tuebingen by Christoph Schaefer and others. Its general use is well documented in [6].

3.1.1 Main SPH concepts

A SPH simulation is composed of many individual SPH particles. Each particle moves through space with a velocity \vec{v} and a mass m . In contrast to particle methods used for N-body simulations or molecular dynamics, SPH particles carry information about continuous variables such as the density ρ or energy e . The particles only act as computational points at which equations from hydrodynamics/continuum mechanics such as the Euler or Navier-Stokes Equations are evaluated. Solving such equations comes down to converting partial differential equations to a system of first order ordinary differential equations in time.

$$\frac{d\vec{y}}{dt} = f(t, \vec{y}(t), A_1, \dots, A_n) \quad (3)$$

In equation 3 \vec{y} is a vector of quantities to be projected forward in time and A_1 through A_n are quantities that are calculated at every step. Once A_1 through A_n are known for every particle and the right hand side of quation 3 can be evaluated, standard integrators such as Runge-Kutta or Predictor-Corrector methods are used to update \vec{y} .

To calculate a quantity A at a particle location, SPH uses a weighted average of A over all particles in the neighborhood:

$$A(\vec{r}) \approx \int A(\vec{r}') W(\vec{r} - \vec{r}', h) d\vec{r}' \quad (4)$$

3.1.2 Smoothing kernel

The kernel function $W(|\vec{r} - \vec{r}'|, h)$ at the particle location \vec{r} depends upon the distance to the other particles and a specific length h called the smoothing length. Most kernels used today have compact support within a radius of h . To ensure normalization of the kernel

$$\int W(\vec{r} - \vec{r}', h) d\vec{r}' = 1 \quad (5)$$

- Smoothing kernel image: 3

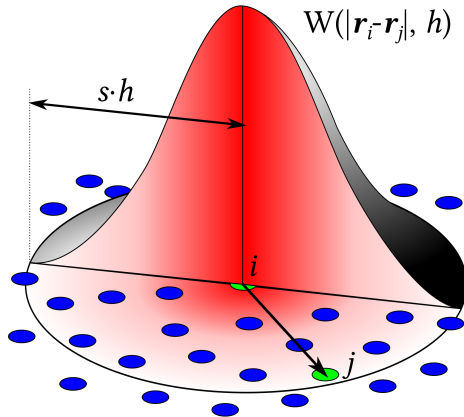


Figure 3: Kernel function [11]

3.1.3 Smoothing length

- can be variable - great strength of SPH - material density and h have to fit together

3.1.4 Artificial viscosity

- what it is - why it is needed

3.2 Initial conditions

3.2.1 Particle setup

- Target basalt halfsphere
- Impactor aluminium sphere
- resolution bound to variable smoothing length
- Uniform macro structure but random micro structure to avoid
- seagen [12] used to create initial conditions

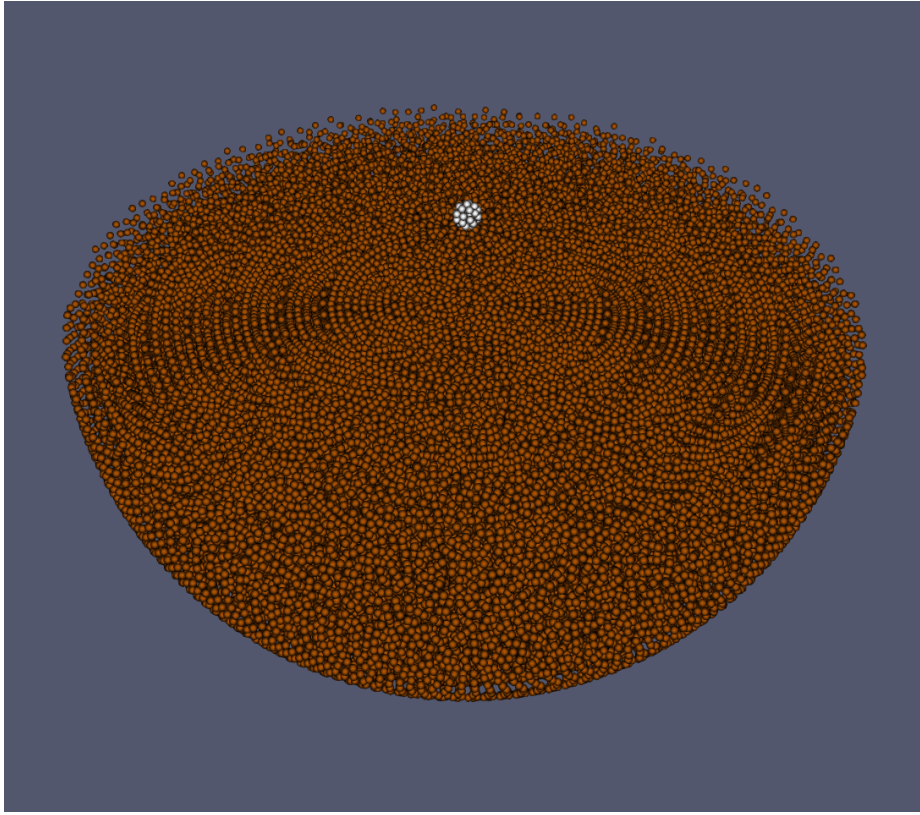


Figure 4: start of example simulation

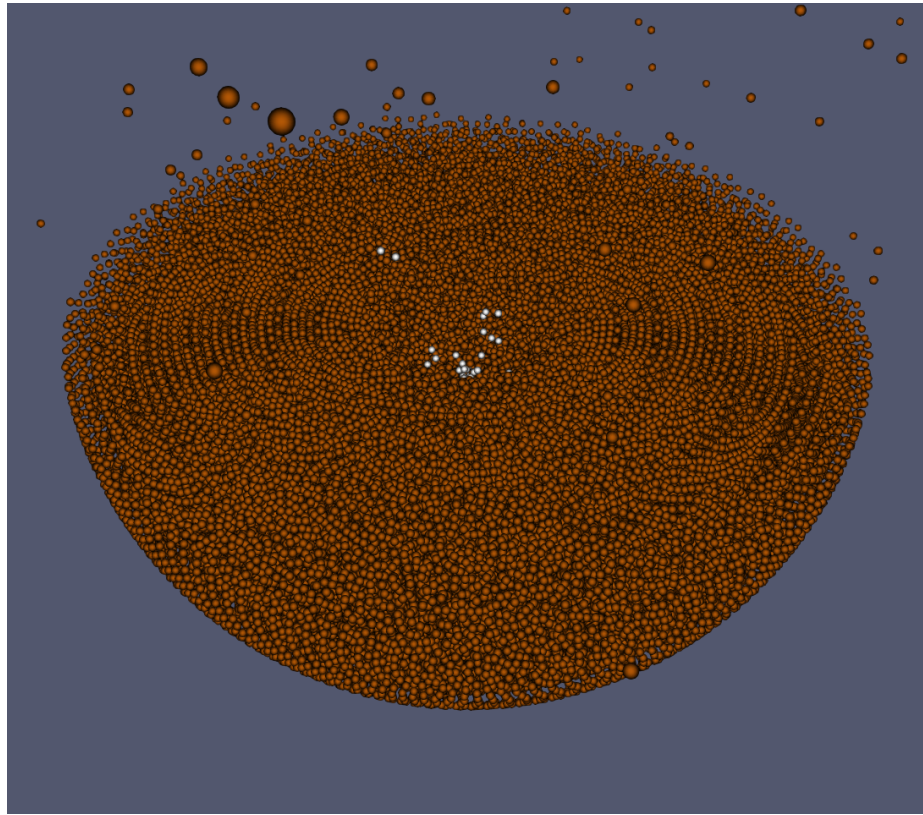


Figure 5: end of example simulation

3.2.2 Material parameters

- variable smoothing length min 0.1 bis max 10.0 - rholimit 0.95

		Target	Projectile
Tillotson EOS	ρ_0	$2.86 \cdot 10^3 g \cdot cm^{-3}$	$2.70 \cdot 10^3 g \cdot cm^{-3}$
	A_T	$2.67 \cdot 10^{10} Pa$	$7.52 \cdot 10^{10} Pa$
	B_T	$2.67 \cdot 10^{10} Pa$	$6.50 \cdot 10^{10} Pa$
	E_0	$4.87 \cdot 10^8 J$	$5.00 \cdot 10^6 J$
	E_{iv}	$4.72 \cdot 10^6 J$	$3.00 \cdot 10^6 J$
	E_{cv}	$1.82 \cdot 10^7 J$	$1.39 \cdot 10^7 J$
	a_T	0.5	0.5
	b_T	1.5	1.63
	α_T	5.0	5.0
Porosity	α_0	varying	not porous
	$p_{elastic}$	$1.0 \cdot 10^6 Pa$	not porous
	$p_{transition}$	$6.8 \cdot 10^7 Pa$	not porous
	$p_{compacted}$	$2.13 \cdot 10^8 Pa$	not porous
	α_e	4.64	not porous
	α_t	1.90	not porous
	c_s	$100.0 m \cdot s^{-1}$	not porous
Strength	cohesive strength Y	varying	$1.0 \cdot 10^9 Pa$
	α_{intact}	0.982793 rad	0 rad
	$\alpha_{damaged}$	0.540419 rad	0 rad
	shear modulus μ	$2.27 \cdot 10^{10} Pa$	$2.69 \cdot 10^{10} Pa$
	bulk modulus K_0	$2.67 \cdot 10^{10} Pa$	$5.23 \cdot 10^{10} Pa$
	yield stress Y_0	$3.5 \cdot 10^9 Pa$	$2.76 \cdot 10^8 Pa$
Fragmentation	Weibull m	16	no damage
	Weibull k	$1.0 \cdot 10^{61}$	no damage
Artificial viscosity	α	1.0	1.0
	β	2.0	2.0

Table 1: Material parameters for basalt target and aluminium Impactor

4 Results

The simulations were run with porosities of 0%, 17%, 33% and 50% and cohesive strengths of 1kPa, 10kPa, 100kPa and 1MPa under impact angles of 0 and 45 degrees. This yields 32 simulations in total.

4.1 Cratering

- qualitative analysis
 - head on

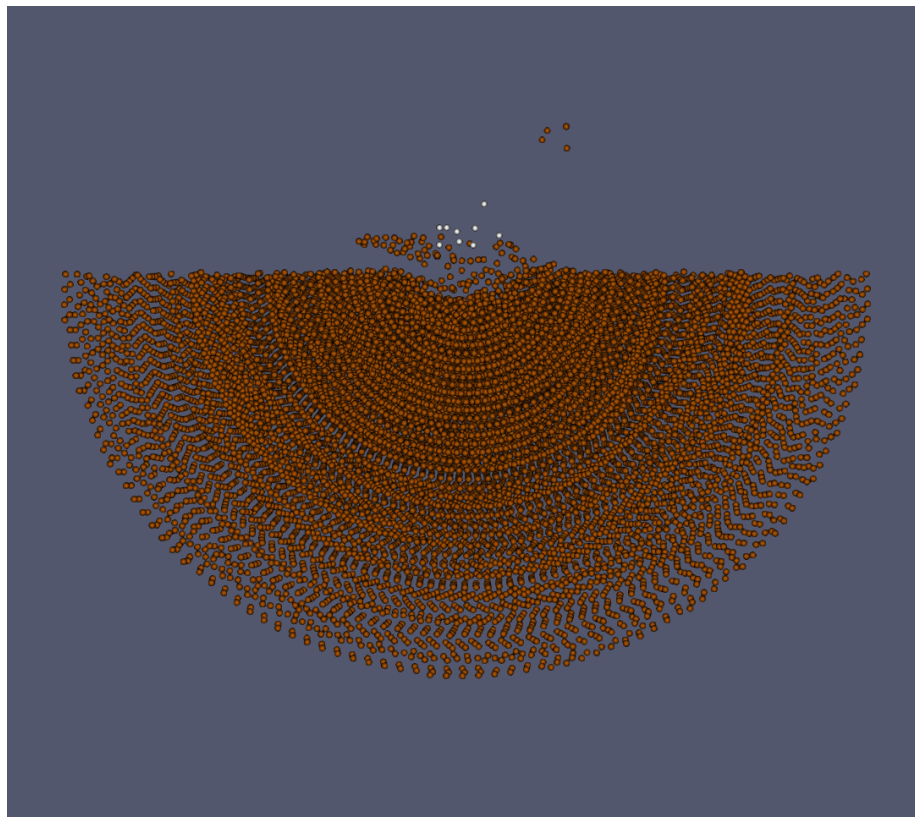


Figure 6: No porosity (0%), high strength ($Y=1\text{MPa}$)

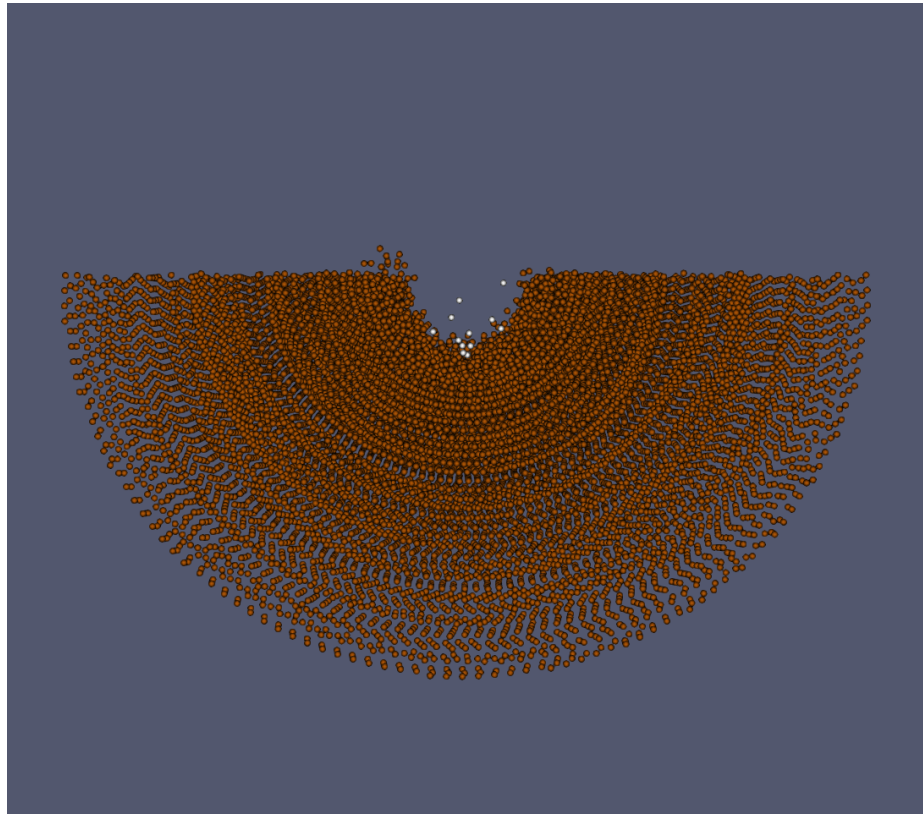


Figure 7: High porosity (50%), high strength ($Y=1\text{ MPa}$)

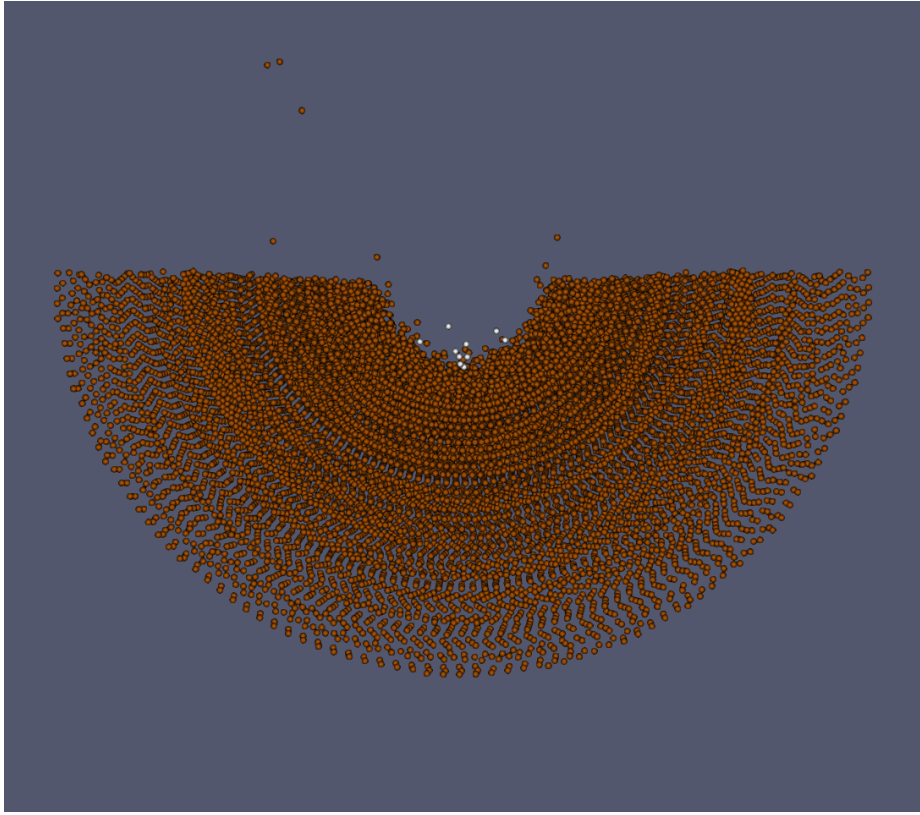


Figure 8: High porosity (50%), low strength ($Y=1\text{kPa}$)

- 45 degrees

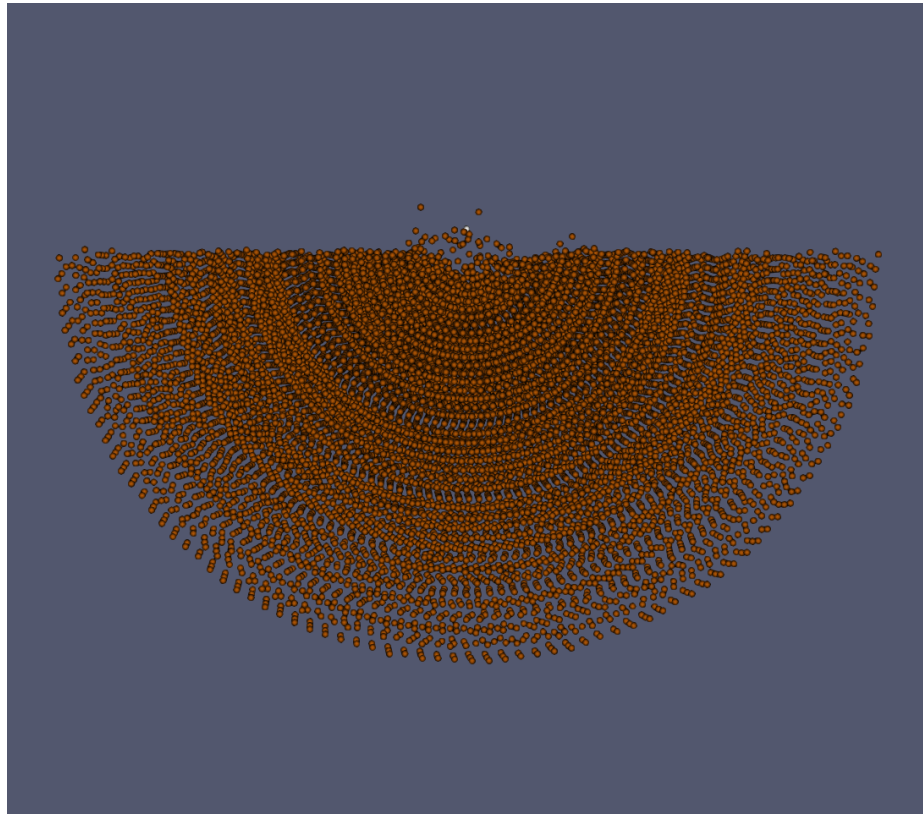


Figure 9: No porosity (0%), high strength ($Y=1\text{MPa}$), 45 degree angle

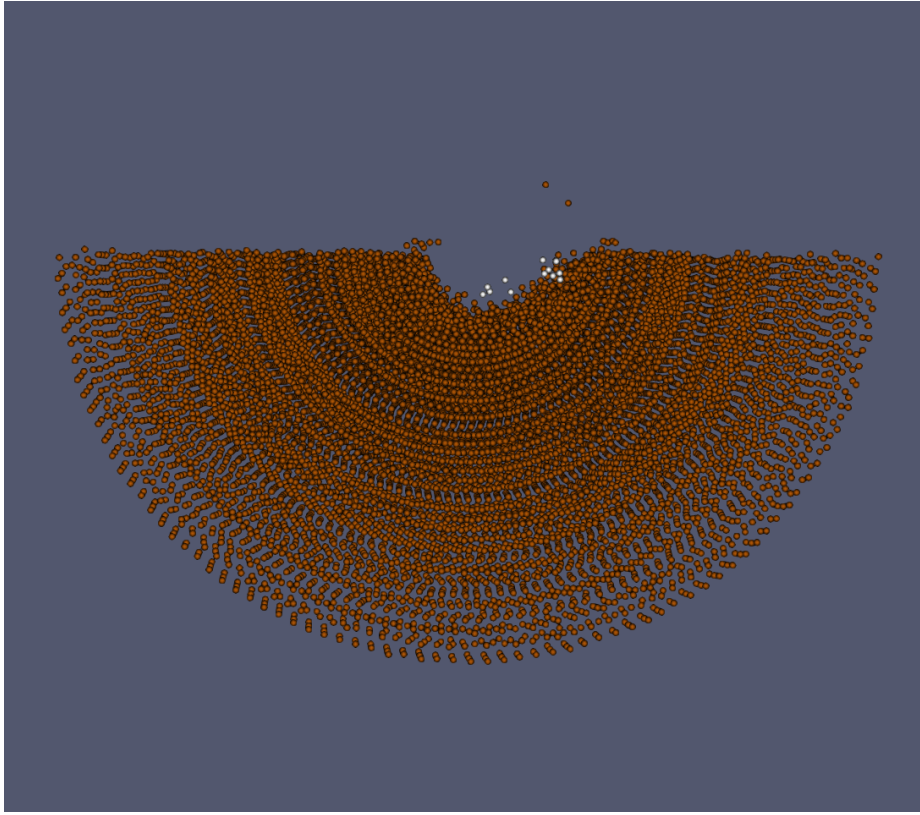


Figure 10: High porosity (50%), high strength ($Y=1\text{ MPa}$), 45 degree angle

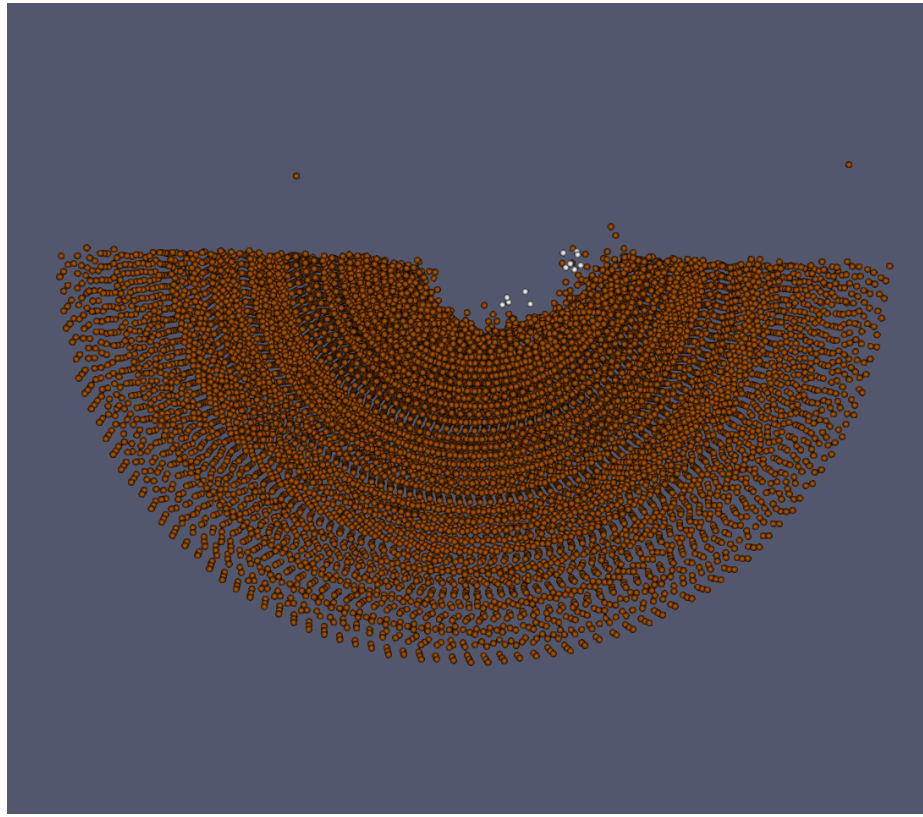


Figure 11: High porosity (50%), low strength ($Y=1\text{kPa}$), 45 degree angle

4.2 Beta factor

- explanation of beta factor

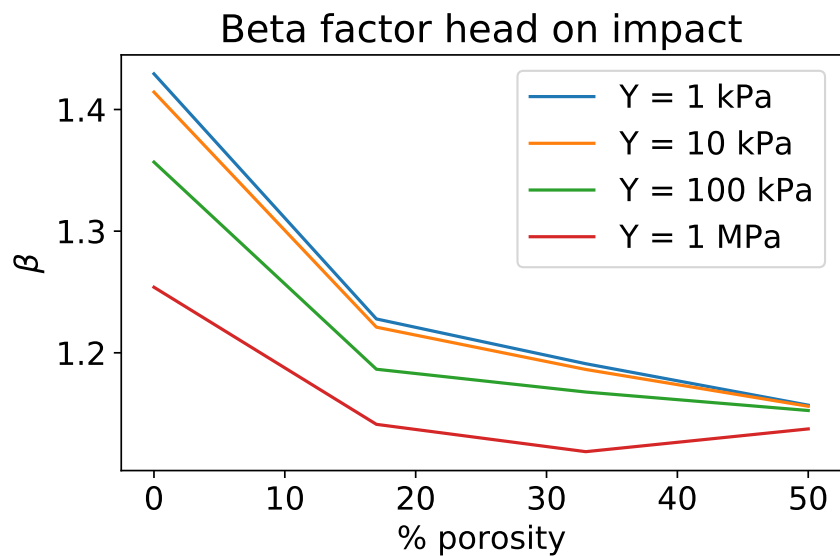


Figure 12: beta factor

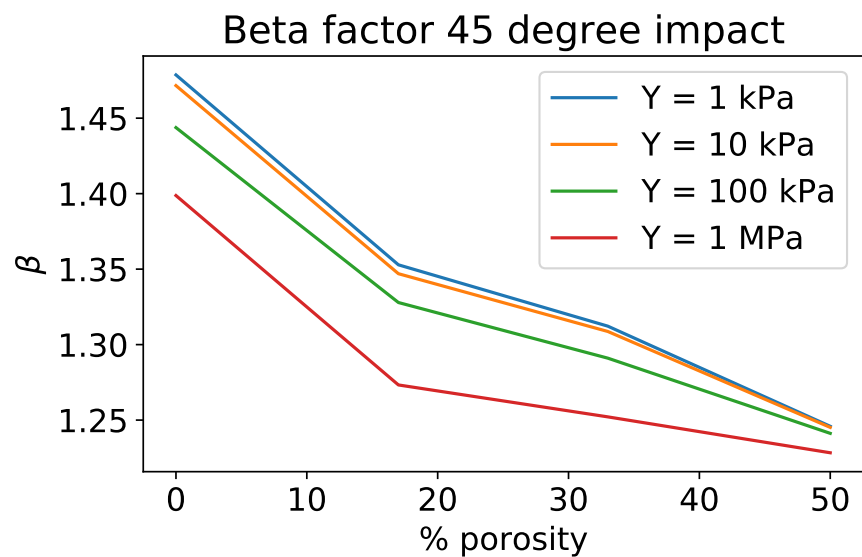


Figure 13: beta factor

- few particles (with highest velocities so the ones that are far away) account for most of the momentum

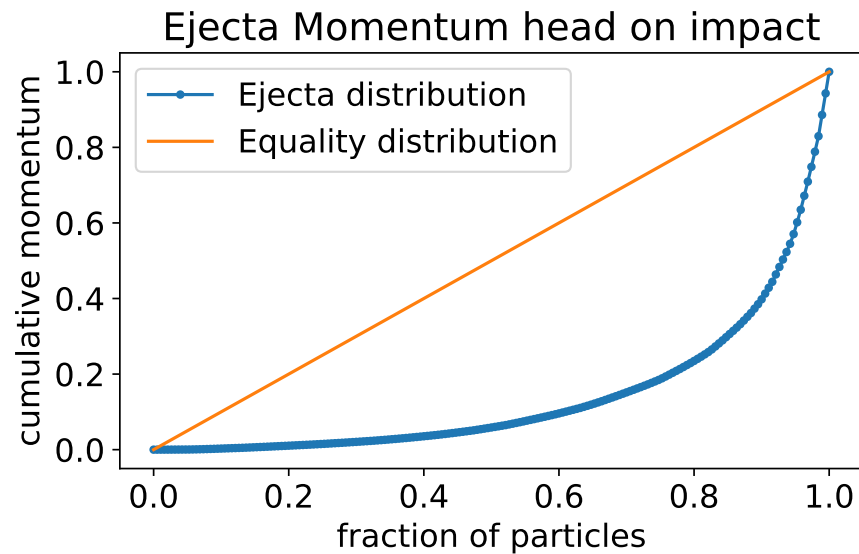


Figure 14: Lorenz curve for momentum distribution head on

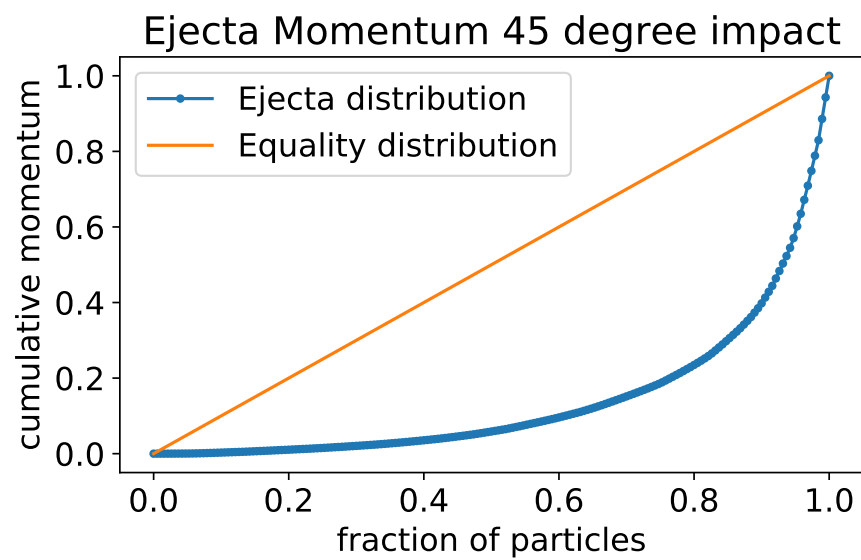


Figure 15: Lorenz curve for momentum distribution 45 degree

5 Discussion

- beta factor lower than Raducan grid based but comparable to Stickle SPH - upper limit beta below 2 because of momentum conservation?? – which inertial system is used for calculation of beta factor in other papers? - tensorial correction not implemented because of timestep getting to small - no real boundary conditions implemented - the whole target shows shift (should not be a problem since we are still in the inertial frame of rest of the target !?)

References

- [1] J. H. Tillotson. “Metallic Equations of State For Hypervelocity Impact”. In: (July 1962), p. 3216.
- [2] R. A. Gingold and J. J. Monaghan. “Smoothed particle hydrodynamics: theory and application to non-spherical stars”. In: *Monthly Notices of the Royal Astronomical Society* 181.3 (Dec. 1977), pp. 375–389. ISSN: 0035-8711. DOI: 10.1093/mnras/181.3.375. eprint: <https://academic.oup.com/mnras/article-pdf/181/3/375/3104055/mnras181-0375.pdf>. URL: <https://doi.org/10.1093/mnras/181.3.375>.
- [3] Gareth Collins, Jay Melosh, and Boris Ivanov. “Modeling damage and deformation in impact simulations”. In: *Meteoritics & Planetary Science* 39 (Feb. 2004), pp. 217–231. DOI: 10.1111/j.1945-5100.2004.tb00337.x.
- [4] Martin Jutzi, Willy Benz, and Patrick Michel. “Numerical simulations of impacts involving porous bodies”. In: *Icarus* 198.1 (Nov. 2008), pp. 242–255. ISSN: 0019-1035. DOI: 10.1016/j.icarus.2008.06.013. URL: <http://dx.doi.org/10.1016/j.icarus.2008.06.013>.
- [5] Martin Jutzi. “SPH calculations of asteroid disruptions: The role of pressure dependent failure models”. In: *Planetary and Space Science* 107 (Mar. 2015), pp. 3–9. ISSN: 0032-0633. DOI: 10.1016/j.pss.2014.09.012. URL: <http://dx.doi.org/10.1016/j.pss.2014.09.012>.
- [6] C. Schaefer et al. “A smooth particle hydrodynamics code to model collisions between solid, self-gravitating objects”. In: *Astronomy and Astrophysics* 590 (Apr. 2016), A19. ISSN: 1432-0746. DOI: 10.1051/0004-6361/201528060. URL: <http://dx.doi.org/10.1051/0004-6361/201528060>.
- [7] A.M. Stickle et al. “Modeling impact outcomes for the Double Asteroid Redirection Test (DART) mission”. In: *Procedia Engineering* 204 (2017). 14th Hypervelocity Impact Symposium 2017, HVIS2017, 24-28 April 2017, Canterbury, Kent, UK, pp. 116–123. ISSN: 1877-7058. DOI: <https://doi.org/10.1016/j.proeng.2017.09.763>. URL: <http://www.sciencedirect.com/science/article/pii/S1877705817343217>.
- [8] Sabina Raducan et al. “The role of asteroid strength, porosity and internal friction in impact momentum transfer”. In: *Icarus* 329 (Apr. 2019), pp. 282–295. DOI: 10.1016/j.icarus.2019.03.040.
- [9] NASA/Johns Hopkins APL. [Online; accessed 22-September-2020]. 2020. URL: https://dart.jhuapl.edu/Gallery/media/graphics/lg/DART-infographic_v4.jpg.
- [10] Wikimedia Commons. *File:SmallAsteroidImpacts-Frequency-Bolide-20141114.jpg* — Wikimedia Commons, the free media repository. [Online; accessed 20-September-2020]. 2020. URL: <https://commons.wikimedia.org/w/index.php?title=File:SmallAsteroidImpacts-Frequency-Bolide-20141114.jpg&oldid=447357435>.

- [11] Wikimedia Commons. *File:SPHInterpolationColorsVerbose.svg* — *Wikimedia Commons, the free media repository*. [Online; accessed 20-September-2020]. 2020. URL: <https://commons.wikimedia.org/w/index.php?title=File:SPHInterpolationColorsVerbose.svg&oldid=446219914>.
- [12] Jacob Kegerreis. *SEAGen*. <https://github.com/jkeger/seagen>. 2020.